THE JOURNAL OF BIOLOGICAL CHEMISTRY VOL. 288, NO. 38, pp. 27638–27645, September 20, 2013

Synthetic Dimeric Aβ(28–40) Mimics the Complex Epitope of Human Anti-Aβ Autoantibodies against Toxic Aβ Oligomers*[S]

Received for publication, February 20, 2013, and in revised form, July 3, 2013 Published, JBC Papers in Press, July 11, 2013, DOI 10.1074/jbc.M113.463273

Andreas M. Roeder[‡1], **Yvonne Roettger**[§1], **Anne Stündel**[§], **Richard Dodel**[§2], **and Armin Geyer**[‡3]

From the [‡]*Faculty of Chemistry, Philipps University of Marburg, Hans-Meerwein-Strasse, D-35032 Marburg and* [§]*Department of Neurology, Philipps University of Marburg, Baldingerstrasse, D-35043 Marburg, Germany*

Background: Human anti-Aβ autoantibodies bind and eliminate toxic oligomers of the Aβ peptide.
Results: Synthetic peptides which contain two properly aligned Aβ(28–40) peptides (called miniamyloids) are bound by human anti-Aβ autoantibodies.
Conclusion: Synthetic miniamyloids mimic the conformational epitope of the transient toxic Aβ oligomers.
Significance: Miniamyloids are expected to become diagnostic tools for the anti-Aβ autoantibodies that are associated with Alzheimer disease.

Covalently linked carboxyl-terminal segments of the β-amyloid peptide (Aβ) were tested for their qualification as minimal conformational epitopes of the naturally occurring human autoantibodies against β-amyloid (nAbs-Aβ). nAbs-Aβ specifically recognize the toxic oligomers of Aβ and not the monomeric or the fibrillar forms of Aβ. The synthetic dimers of Aβ(28–40) described herein mimic the toxic Aβ oligomers but are not kinetic intermediates with uncertain compositions. CD spectra identified a surprisingly rich conformational behavior of selected miniamyloids. We observed a highly cooperative conformational transition of β-sheet to α-helix upon the addition of the helix enforcing co-solvent hexafluoroisopropanol. The CD curves of dimer 9 resembled, in a completely reversible manner, the CD spectra measured during the irreversible fibrillation of the parent Aβ(1–40). Synthetic peptide epitopes with high affinities for nAbs-Aβ are needed to identify the physiological roles of nAbs-Aβ and are promising epitopes for vaccination experiments.

Alzheimer disease is a progressive neurodegenerative disorder and the most common cause of adult-onset dementia (1, 2). Naturally occurring human autoantibodies against β-amyloid (nAbs-Aβ)[4] can bind to and may eliminate soluble oligomeric β-amyloid peptides (Aβ) (3–5). nAbs-Aβ interfere with Aβ toxicity and have been shown to improve memory performance in a transgenic amyloid precursor protein animal model (6). Although the epitope region was identified in the C-terminal region of Aβ, it is unclear how nAbs-Aβ specifically recognize toxic Aβ oligomers and distinguish them from unbound monomeric Aβ or fibrillar Aβ. The soluble Aβ oligomers are transient intermediates in the Aβ fibrillation process. This aggregation is practically irreversible under physiological conditions, thus complicating the spectroscopic identification of the topological differences that separate toxic Aβ oligomers from other aggregation states of Aβ. More precise data about the distribution of oligomers or the distribution of binding affinities by the nAbs-Aβ are not available. Although numerous spectroscopic studies have focused on either monomeric or fibrillar Aβ, the toxic intermediate Aβ oligomers remain incompletely characterized due to their fleeting character. The idea that there are significant structural differences between the monomeric, fibrillar, and the toxic intermediate oligomers of Aβ is corroborated by the existence of selective antibodies against particular aggregation states of Aβ (7). In the current study, nAbs-Aβ are critical for helping to identify the toxic Aβ epitope from a pool of synthetic compounds without microheterogeneity and without being kinetic intermediates.

Spectroscopic analyses identified various conformational states of Aβ, which were strongly dependent on the preparation method and the solvent environment (8, 9), yet the cooperativity of a reversible folding/unfolding process was not analyzed previously. Soluble monomeric Aβ is best conceived as a pool of rapidly equilibrating conformers, which are mainly helical with a strong tendency to form β-sheets at the C terminus (10). This conformational variability is demonstrated in the crystal structure of Aβ28–42 linked to the C terminus of ribonuclease HII from *Thermococcus kodakaraensis*, wherein the peptide displays a β-sheet conformation with a turn encompassing amino acids 35–38 (11). However, the complex of monomeric Aβ(1–40) bound to a host-protein (affibody ZAβ3) forms a β-hairpin composed of amino acids 17–36 with a turn at position 24–28 (12). Herein, the C terminus is less ordered, but a backfolding of the peptide chain was again observed.

* This work was supported by the Deutsche Forschungsgemeinschaft.
[S] This article contains supplemental Figs. S1–S4.
[1] Both authors contributed equally to this work.
[2] To whom correspondence may be addressed: Dept. of Neurology, Philipps-University Marburg, Baldingerstrasse, 35043 Marburg, Germany. Tel.: 49-6421-58-66251; Fax: 49-6421-58-65474; E-mail: dodel@med.uni-marburg.de.
[3] To whom correspondence may be addressed: Fachbereich Chemie, Philipps-Universität Marburg, Hans-Meerwein-Strasse, 35032 Marburg, Germany. Tel.: 49-6421-28-22030; Fax: 49-6421-28-22021; E-mail: geyer@staff.uni-marburg.de.
[4] The abbreviations used are: nAbs-Aβ, naturally occurring human autoantibodies against β-amyloid; Aβ, amyloid β; DMF, *N,N*-dimethylformamide; HFIP, hexafluoroisopropanol.

Despite several structural investigations driven by the considerable pathological significance of the toxic form of Aβ (13), our understanding of the physico-chemical properties of the toxic nAbs-Aβ oligomers is incomplete (14). Peptide models of the aggregation process have identified common properties of the so-called cross-β-peptides, but drawing analogies between peptides with different amino acid compositions is error prone. It would be desirable to characterize individual oligomerization states of Aβ individually, yet equilibration between the states cannot be prevented. Covalent tethering by a disulfide (13, 15–17) or an organic scaffold (18) yielded dimers synthesized to resemble the first aggregation state. However, the dimers are inclined to form fibrils with themselves and eventually even more effectively than the parent Aβ. We believed it was critically necessary to actively prevent further aggregation of the covalently linked Aβ strands. A surplus of cationic charges proved to be effective for avoiding uncontrolled aggregation. Potential unspecific effects were excluded by investigating pairs of monomeric and dimeric Aβ peptides that bear similar charge patterns. In the following study, we describe the spectroscopic properties, nAb-Aβ-specific affinities, and toxicity profiles of miniamyloids, which are well behaved organic molecules mimicking key features of toxic Aβ. Soluble peptides that mimic the conformational epitope of the transient toxic Aβ oligomers are suggested as diagnostic tools for the identification of anti-Aβ autoantibodies, which are associated with Alzheimer disease.

EXPERIMENTAL PROCEDURES

Polypeptide Synthesis—The synthesis of the miniamyloids was accomplished by automated solid phase peptide synthesis using the Fmoc strategy. Peptide synthesis was performed in a 0.1-mm (monomers) or 0.05-mm (dimers) scale on 2-chloro-2-trityl-polystyrene-resin using an Advanced Chemtech APEX 396. After preloading the resin with the first Fmoc amino acid, the synthesis was performed as described below: a, swelling in 2.5 ml of *N*,*N*-dimethylformamide (DMF) for 15 min; b, 2× deprotection with 2.0 ml of 20% piperidine solution in DMF (first for 5 min and second for 10 min); c, 3× washing with 2.0 ml of DMF; d, 2× washing with 2.0 ml dichloromethane; e, 2× washing with 2.0 ml of DMF; f, swelling in 2.5 ml of DMF for 5 min; g, coupling with 3.0 eq of 2-(1*H*-benzotriazole-1-yl)-1,1,3,3-tetramethyl-uronium hexafluorophosphate/1-hydroxybenzo-triazole/fluorenylmethoxycarbonyl protected amino acid and 6.0 eq of diisopropyl-ethylamine for 60 min; h, 2× washing with 1.5 ml of DMF; i, coupling with 1.0 eq of the reagents from g and 3.0 eq of diisopropylethylamine for 60 min; j, 2× washing with 1.5 ml of DMF. Repeating the steps b–j with the resin and the appropriate amino acids finally yielded the desired peptide. Removal of all side chain protecting groups and cleavage from the resin was performed by agitating the resin in trifluoroacetic acid/H_2O/1,2-ethanedithiol/triisopropylsilane (94:2.5:2.5:1) for 30 min. Precipitation and washing with diethyl ether yielded the trifluoroacetic acid salt of the peptide, which was redissolved in water and obtained as a powder after lyophilization. The branching of the peptide strands of the dimeric miniamyloids was achieved by incorporating double Fmoc-protected lysine and subsequent peptide elongation at the α- and ϵ-nitrogen.

Mass Spectrometry—MALDI-TOF MS spectra were obtained from a Bruker Ultraflex mass spectrometer and dihydroxybenzoic acid matrix.

NMR Spectroscopy—The NMR spectra were recorded on a Bruker Avance DRX 600 spectrometer. Peptides were freshly solubilized in dimethyl sulfoxide-d6 or 10 mM potassium hydrogen phosphate buffer (pH 7)/D_2O (5:1) at 30 °C under ultrasonication and were investigated directly. The aqueous samples were centrifuged (10,000 rpm, 5 min) prior to use. Water suppression was achieved by excitation sculpting with gradients (double Watergate DPFGSE sequence). Signal assignment was achieved using two-dimensional homonuclear (COSY, TOCSY, and NOESY) and heteronuclear (HSQC amd HMBC) experiments.

CD Spectroscopy—CD spectra were obtained using a JACSO S-810 spectrometer. A quartz glass cuvette with 1-mm optical path lengths was used. The spectra were recorded at 4 °C between 190–270 nm with a bandwidth of 1 nm, a response time of 2 s, and a scanning speed of 50 nm/min. Each spectrum represents the average of five consecutive scans. All peptides were freshly solubilized in filtered 10 mM potassium hydrogen phosphate buffer (pH 7), bidistilled water, or HFIP to a concentration of 0.12 mm at 30 °C under ultrasonication. The samples were directly investigated.

Surface Plasmon Resonance Analysis—The binding kinetics of nAbs-Aβ to immobilized amyloid peptides were analyzed using the XPR36 ProteOn system (Bio-Rad). Peptides were immobilized on a ProteOn GLH sensor chip (Bio-Rad) using an amine coupling kit (Bio-Rad). All steps were carried out at 25 °C with a flow rate of 30 μl/min and 5 min of contact time. Following activation of GLH chips with 1-ethyl-3-(3-dimethylaminopropyl)carbodiimide and 3-sulfo-*N*-hydroxysuccinimide solution, amyloid peptides at a concentration of 100 μg/ml in 10 mM acetate buffer pH 4.5 were immobilized. Residual binding sites were deactivated by ethanolamine injections. Phosphate-buffered saline (pH 7.4) containing 0.005% Tween 20 (PBS-T) was used as running buffer. Kinetic response data were collected for nAbs-Aβ at five concentrations (6000, 3000, 1500, 750, and 375 nM in PBS-T) injected simultaneously in parallel channels at a flow rate of 100 μl/min for a 1-min association phase followed by a 10-min dissociation phase at 25 °C. All data were analyzed by the interspot reference function of the XPR36 software (Bio-Rad). Kinetic constants (association rate (k_{on}), dissociation rate (k_{off}), maximal response units at equilibrium (R_{max}), and the K_D value) were calculated based on highest antibody concentration (6000 nM) using a Langmuir Kinetic model provided by the XPR36 ProteOn software. After each analysis, the sensor surface was regenerated by a two-step cleaning via injection of glycine buffer (pH 2.5) followed by phosphoric acid (each 100 μl/min for 120 s).

Dot Blot—The different Aβ preparations were obtained according to established methods. Briefly, monomers were prepared by generating a 150 μM peptide solution in 10% dimethyl sulfoxide and 90% H_2O following 15 min of sonication to minimize spontaneous oligomerization. Oligomers were prepared according to a standardized protocol as published recently (33). Fibrils were obtained by preparing a 150 μM peptide solution in 10% dimethyl sulfoxide, 90% H_2O following incubation for 48 h

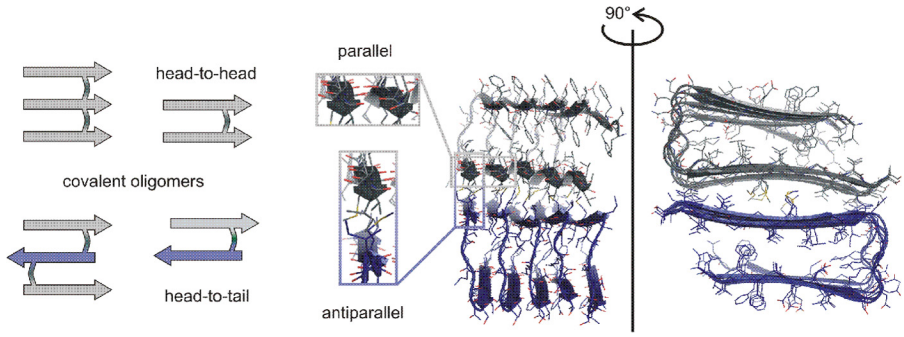

FIGURE 1. **The aligned *arrows* depict possible linkages between the Aβ peptide segments.** These covalently linked oligomers are named miniamyloids (*left*). Head-to-head dimers and head-to-tail dimers of the C-terminal part of Aβ are the minimal structural representatives of the parallel and antiparallel contacts of fibrous Aβ, respectively (*middle*). Both relative orientations are observed for the C-terminal epitope of Aβ in the proposed models (*right* (Ref. 19)) of Aβ fibrils (Ref. 24).

at 37 °C. Dot blots were performed by applying 0.02 nmol of peptide solution to a nitrocellulose membrane. Membranes were blocked using Roti®-Block (Roth) and primary antibodies (6E10 antibody 1:2000 dilution; 6F/3D antibody, 1:1000 dilution; nAbs-Aβ, 1 μg/ml or nAbs-**9a** 1 μg/ml) were applied, followed by incubation with the secondary antibody (HRP-conjugated antibody against human IgG, Pierce) at a final concentration of 0.8 ng/ml. Titration experiments started with 0.056 nmol of peptide per dot up to 0.0035 nmol per dot in a 1:2.5 dilution series.

Antibody Isolation—Naturally occurring antibodies were prepared from intravenous immunoglobulins (a gift from Octapharma AG, Interlaken, Switzerland) as described previously (6). Briefly, disposable chromatography columns were packed with UltraLink iodoacetyl gel (Thermo Scientific) and Cys-Aβ1–42 (or Cys peptide **9a**) was covalently attached to the matrix according to the manufacturer's instructions. Intravenous immunoglobulins (1:1 in PBS) were loaded on the columns overnight at 4 °C. Following several washing steps, bound Aβ antibodies were eluted using 0.1 M glycine buffer, pH 2.8. To maintain the integrity of the antibodies, a neutral pH was immediately adjusted after elution by adding the appropriate amount of Tris-HCI or glycine buffer.

Neurotoxicity Assay—Primary mice neuronal cell cultures were prepared from E13 Swiss Webster mice embryos. Cortices were isolated and collected in Leibovitz L-15 medium (Sigma-Aldrich). The cortices were homogenized and resuspended in Neurobasal®. A medium supplemented with B-27® supplement (2%), penicillin/streptomycin (1%), and L-glutamine (1%). Cells were grown on polyethylenimine-coated 48-well plates for 5 days. Peptides were dissolved in H_2O with a final peptide concentration of 150 μM. Cells were treated with a final peptide concentration of 5 μM for 48 h. Toxicity was measured using the methyl thiazolyl diphenyltetrazolium bromide assay. Briefly, cells were incubated for 1 h at 37 °C with methyl thiazolyl diphenyltetrazolium bromide (0.5 mg/ml). Cells were permeabilized with dimethyl sulfoxide for another 30 min, and absorbance was measured at 570 nm. All measurements were done at least in duplicates.

RESULTS

Peptide Design—The relative orientation of the peptides in fibrillar Aβ (19–23) served as a template for the design of the synthetic miniamyloids. Fig. 1 identifies two different supramolecular contact sites for the C-terminal amino acids, ^{28}KGAIIGLMVGGVV^{40}, in the solid-state structure of fibrillar Aβ.

On the assumption that either the parallel or the antiparallel relative orientation of two β-strands mimics the conformational (discontinuous) epitope of nAbs-Aβ, we tested different linkages and different solubilizing groups (6, 25). Bifurcated peptides with Lys as the branching amino acid proved superior to other types of linkages. Additional Lys, Arg, and Glu residues were added as solubilizing groups and were separated by one aminohexanoic acid. The dimeric peptides were rightfully compared with the monomeric peptides bearing the same solubilizing groups. Table 1 lists 10 monomeric, seven dimeric, and one tetrameric peptide (more peptides are shown in supplemental Fig. S3). The compounds differed by the positioning of the additional charges on either end of the peptide; some are clustered and separated by a spacer, and others are distributed throughout the individual peptide strands.

^{1}H NMR—The solubilizing effect of adding additional charged side chains to Aβ peptides is obvious by ^{1}H NMR (Fig. 2) (26). The monocationic Aβ(28–40)-ϵ-aminohexanoic acid peptide (**1**), which already bears the C-terminal ϵ-aminohexanoic acid linker and is employed in the synthesis of the branched peptides, is nearly undetectable due to aggregation. Addition of a single Lys (**2**) does not give an adequately resolved ^{1}H NMR, whereas three Lys added to monomeric Aβ (**3**) or two Lys per strand of dimeric Aβ (**4**) yield high-resolution spectra due to the breakdown of aggregates. The compounds are completely soluble and remain dissolved over time, showing spectroscopic properties independent of the incubation time. No concentration dependence was observed for the ^{1}H NMR chemical shifts or in the CD spectra. Although the ^{1}H NMR spectra of peptides **3**-**18** are well resolved in aqueous buffer solution, showing only a slight signal dispersion among the investigated peptides and the time averaged rotating frame nuclear Overhauser enhancements, and the ^{3}J coupling constants are indicative of conformational averaging for the relevant NMR time scales (data not shown).

Circular Dichroism Measurements—CD spectroscopy can distinguish between two groups of miniamyloids that either show a broad minimum at a mean residue ellipticity of ~220

TABLE 1

Spectroscopic characterization and affinity studies of miniamyloids

The net charge is calculated at physiological pH. The minimum in the CD spectrum was used for the calculation of the β-sheet content. The binding properties for surface plasmon resonance are included as R_{max}. The K_D values were calculated from the SPR binding properties. The toxicity of the synthetic miniamyloids was tested in primary cortical neurons with a viability assay (MTT assay 3-(4,5-dimethylthiazol-2-yl)-2,5-diphenyltetrazolium bromide). The viability for each peptide was normalized to the viability of untreated cells.

no.	peptide sequence	net charge	Θ_{min} (10^3 deg cm^2 dmol^{-1})	β-sheet (%)	R_{max} (RU)	K_D (10^{-8} mol^{-1} L)	Viability (%)
1		1+	-	-	-	-	-
2		2+	-	-	-	-	-
3		4+	-1.23[b]	0	27	291	96
4	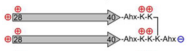	7+	-8.19[b]	56	38	35	21
5		3+	-4.67[b]	23	22	126	86
6	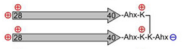	5+	-6.65[b]	77	149	55	28
7	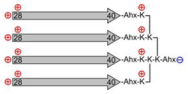	11+	-9.26[a]	98	138	21	30
8		6+	-0.48[b]	0	-[c]	-[c]	96
9	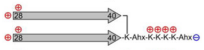	7+	-8.99[a]	73	40	21	47
10		6+	-1.29[b]	13	-[c]	-[c]	84
11	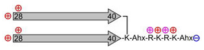	7+	-8.03[b]	86	170	67	24
12		5+	-2.93[b]	34	194	6	91
13		6+	-8.92[b]	76	63	34	97
14	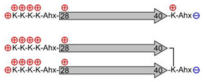	11+	-7.07[a]	95	105	23	40
15		6+	-0.43[b]	24	24	12	91
16	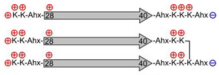	11+	-3.42[b]	16	39	30	41
17	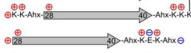	2+	-3.89[a]	22	30	9	105
18	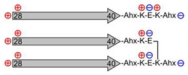	3+	-6.69[b]	77	191	17	97

[a] λ = 216 nm.
[b] λ = 218 nm.
[c] Affinity was below the detection limit. The residual percent to hundred in the structural designation are of α-helical character (1–4%).

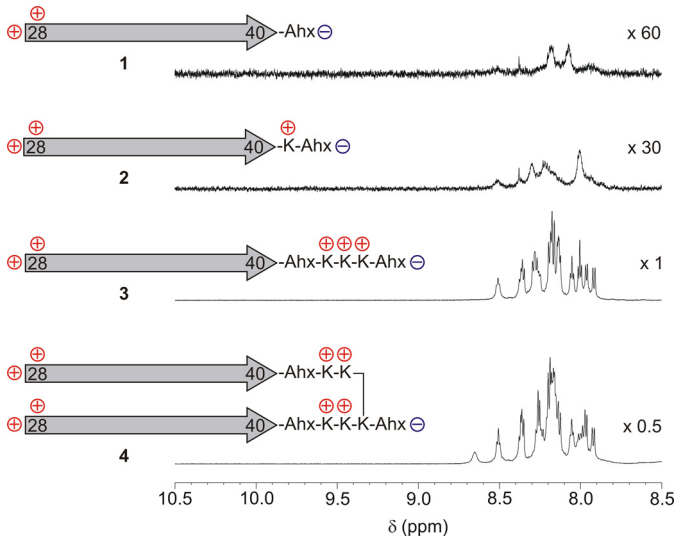

FIGURE 2. **Expansions of the ^{1}H NMR spectra (600 MHz, 10 mm KH_2PO_4 buffer pH 7, 300 K) of peptides 1–4.** Positively and negatively charged groups are indicated on the Aβ(28–40) epitope, which itself is represented by an *arrow*. Despite the comparable sample concentrations, nearly no detectable ^{1}H NMR signal was observed for **1,** and only broad signals were observed for **2**, whereas **3** and **4** yielded high-resolution spectra. The signal assignments for **3** are given in the supplemental data.

nm (Fig. 3*a*) or an intense minimum below 200 nm and a small negative shoulder at ~220 nm (Fig. 3*b*). The value at 220 nm is included in Table 1. Minor structural variations between the peptides have considerable influence on the CD spectra. The intense negative band below 200 nm was similar to the CD of freshly prepared Aβ, characterized as a random coil, whereas the spectra with the weaker minimum above 215 nm resembled the spectrum of Aβ after several weeks of fibrillation as β-sheets (see Fig. 5 in Ref. 28). All dimeric and only one monomeric peptide belong to the first group, which show CD spectra very similar to freshly prepared Aβ(1–40).

Upon lowering the pH below 5.8, the β-sheet forming peptides (shown in Fig. 3*a*) unfolded cooperatively. The pH titration of peptide **9** is presented in Fig. 4. The second group of peptides (shown in Fig. 3*b*) showed no signs of cooperative changes of spectroscopic properties as expected for unfolded peptides with random coil conformations.

The temperature dependence of CD is inconclusive and seems to be influenced by unspecific hydrophobic effects observed as reversible clouding of the samples at elevated temperatures. However, a very clear picture was obtained upon titration with HFIP. As demonstrated, the complete range of known conformational polymorphism of Aβ (29–31) was traversed in a reversible manner for miniamyloid **9** during this titration (Fig. 5). The deconvolution of the complete titration range during HFIP addition shows three separate structural motifs for **9** (32). From what most likely began as a β-turn in pure buffer, a β-sheet formed uniformly upon the addition of 10% HFIP. At only 20% HFIP, the spectrum showed greater than 70% α-helical content. Once HFIP content was >50%, the helix finally unfolded into a random coil. Strongly coordinating alcohols such as HFIP are expected to induce α-helices (32). This property was employed to characterize the β-sheet structure by observing its stability against the denaturing solvent HFIP (supplemental Fig. S1). The maximal β-sheet content is included in Table 1. With the exception of **13**, all of the monomeric peptides had low β-sheet content, whereas several dimers reached values of ~90% β-sheet character, and the tetramer **7** showed 98%. The corresponding pairs of dimers and monomers exhibited higher β-sheet content for the dimer. This result proved that it is possible to covalently align Aβ fragments and prevent further aggregation to the fibrillar structures (supplemental Fig. S2).

Antibody Binding—The N-terminal Aβ antibody 6E10 is known to recognize Aβ regardless of its aggregation state (*i.e.* monomers, oligomers, and fibrils), whereas 6F/3D binds only oligomeric states (Fig. 6*a*). nAbs-Aβ bind a discontinuous (conformational) epitope that neither monomers nor fibrils only oligomers of Aβ can offer. Peptide **9** was selected as a ligand for nAbs-Aβ for affinity chromatography. The ability of the miniamyloids to mimic Aβ oligomers is qualified by their ability to extract natural antibodies from blood serum preparations. To test this theory, we synthesized miniamyloid **9a** (Fig. 6). **9a** differs from **9** because of its C-terminal cysteine, which can serve

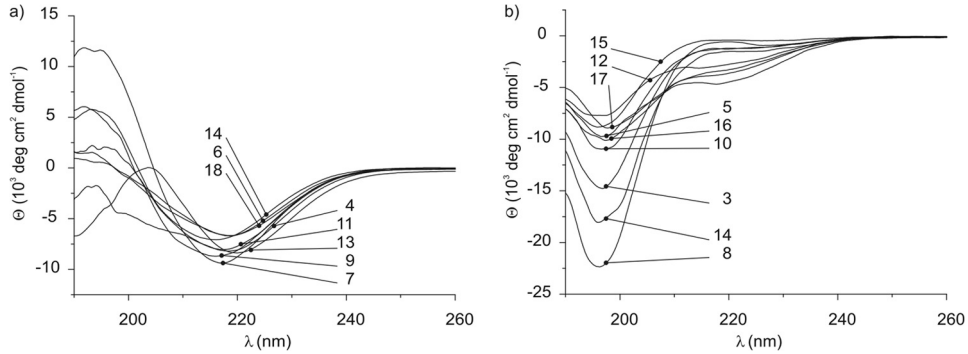

FIGURE 3. **Circular dichroism spectra of the peptides listed in Table 1 and supplemental Fig. S3 (10 mM KH_2PO_4 buffer, pH 7, 4 °C).** The miniamyloids are divided in two groups according to their CD curves (mean residue ellipticities). *a*, dimeric miniamyloids, **4**, **9**, **11**, **13**, **14**, **18**, and tetramer **7** exhibit a minimum between 216 and 218 nm. Additionally, monomer **13** fits into this group. *b*, all other monomers, **3**, **5**, **8**, **10**, **12**, **15**, and **17**, appear to be unstructured with a strong negative band below 200 nm. The dimers that fall into this group have several N-terminal charges (peptides **14** and **16**). More control peptides are listed in the supplemental data. The monomeric peptides, **1** and **2**, are not included because they were not soluble.

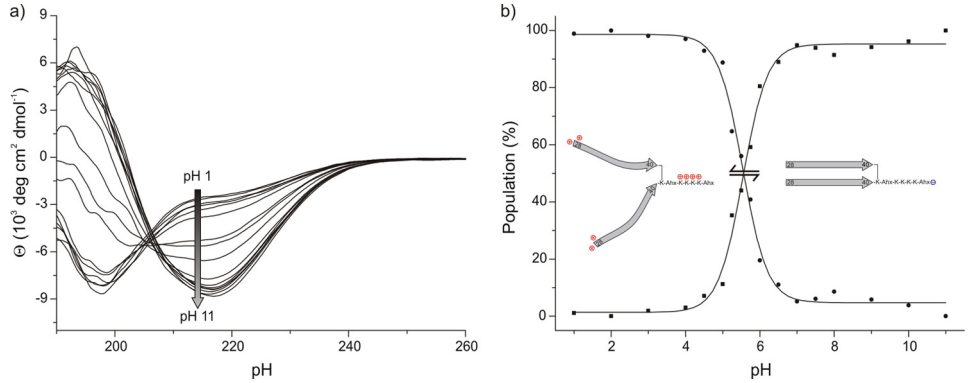

FIGURE 4. **The CD spectrum of 9 varies with pH.** *a*, the sign inversion of the maximal mean residue ellipticity at ~190 nm and the concomitant decrease of the signal intensity at ~215 nm in the opposite direction identifies an isosbestic point at 205 nm upon increasing the pH from 0 to 11. *b*, population analysis of the CD values at 190 and 215 nm showed a sigmoidal pH dependence (*right*). The β-sheet appears to be formed cooperatively at approximately pH 5.8. The ^{1}H NMR is not significantly influenced by pH (not shown).

as a linker to an affinity chromatography column (iodoacetyl matrix; see also "Experimental Procedures"). Therefore, we were able to isolate specific antibodies from intravenous immunoglobulins (intravenous immunoglobulin) preparations using miniamyloid **9a** as a capture molecule. Those isolated antibodies (nAbs-**9a**) recognized Aβ oligomers with affinities comparable with that of nAbs-Aβ (Fig. 6*b*). The semi-quantitative dot blots served as a basis for confining the peptide library to dimers, which are linked in a parallel relative orientation (data not shown). Other tethering concepts were not tested and are therefore not part of this work (25).

Surface Plasmon Resonance Measurements—Surface plasmon resonance allows for an appropriate quantitative affinity measurement. After immobilization of the peptides (Table 1 and supplemental Fig. S3) to the GLH sensor chip surface, nAbs-Aβ was applied in a concentration of 6 μM. The binding was visualized by a typical surface plasmon resonance sensorgram, as shown in supplemental Fig. S4. According to the R_{max} values, the peptides were differentiated into structures of higher or lower affinity. To exclude false positives, a non-toxic, low-affinity monomeric peptide was a prerequisite. Monomers that were recognized by the antibody (**12**, **13**, **15**, and **17**) were regarded as false positives that form supramolecular oligomers in the presence of the antibody and therefore show affinities similar to the corresponding dimers (**14**, **16**, and **18**). These peptides bear N-terminal charged groups (**12**, **13**, and **14**), charged groups on both ends (**15** and **16**), or C-terminal amphiphilic groups (**17** and **18**). Only the peptides with C-terminal cationic charges showed good activities. They were subdivided into miniamyloids with separated cationic charges on each Aβ(1–40) peptide fragment (**4**, **6**, and tetramer **7**) and miniamyloids with the same charged groups clustered together near the C-terminal of the branching Lys (**9** and **11**). Control peptides with anionic groups, or longer expansions of Aβ, or D-configurated amino acids are listed as supplemental data.

Toxicity—Oligomeric Aβ(1–40) was obtained according to the incubation protocol previously published by Kayed *et al.* (33). To investigate the different characteristics of monomeric and dimeric peptides in terms of toxicity, primary mouse cortical neurons were exposed to the peptides preparations, and the viability of the cells was assessed by the methyl thiazolyl diphenyltetrazolium bromide assay. The viability for each peptide was normalized to the viability of untreated cells. Results are included in Table 1. In our experiments, we aimed to establish pairs of peptides (miniamyloids) that have comparative properties to monomeric and oligomeric Aβ(1–40) without exhibiting the effect of Aβ(1–40) of further aggregation into fibrils. Here, we aimed to compare the capability of the miniamyloids to induce toxicity on primary neurons. The treatment of primary neurons with oligomeric Aβ(1–40) resulted in a

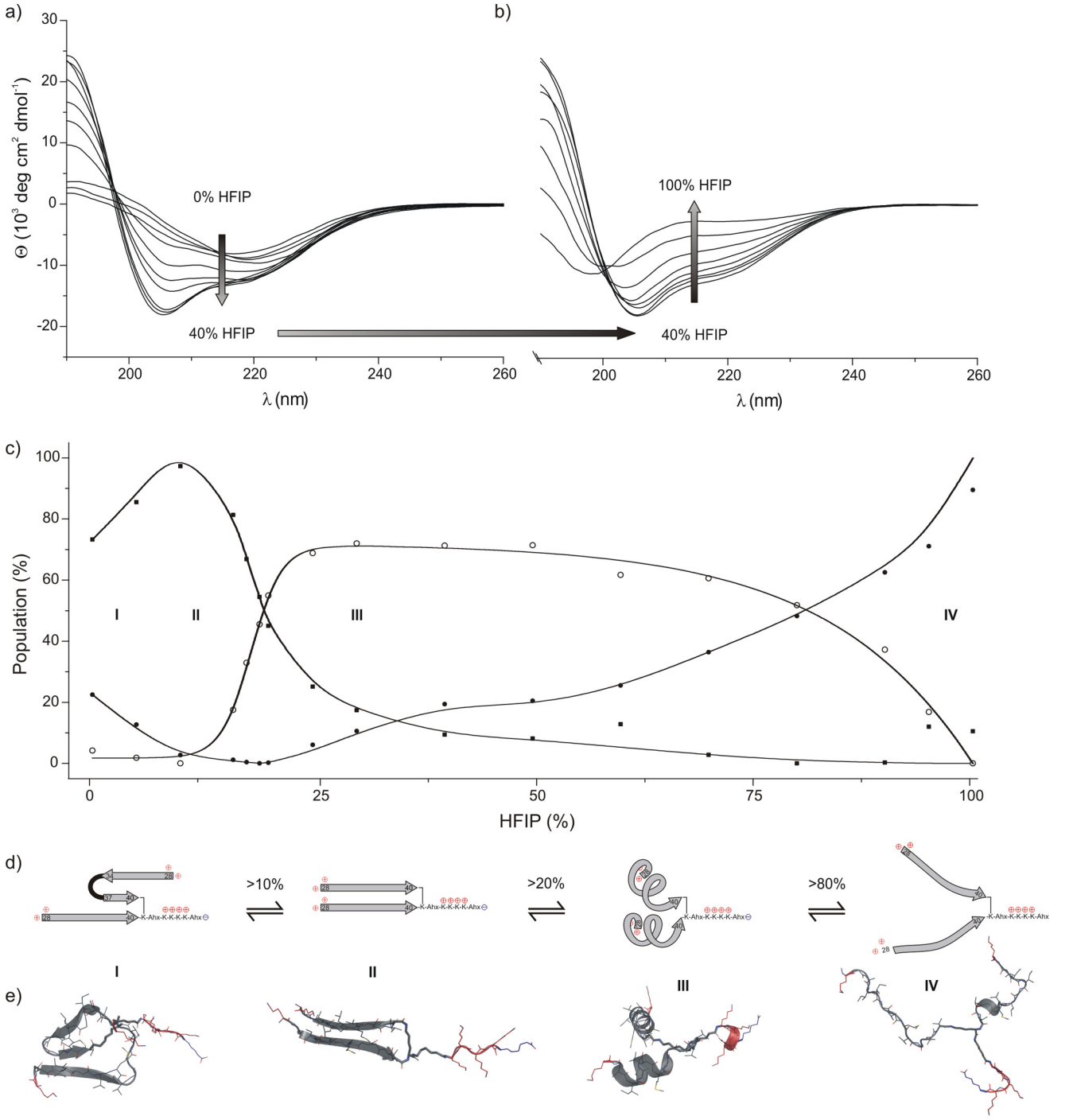

FIGURE 5. Shown is the HFIP titration of miniamyloid 9 in KH_2PO_4 buffer between 0 and 40% HFIP (*a*) and in between 40 and 100% HFIP (*b*). *c*, a population analysis identifies different conformational states of **9**. *d*, schematic representation of the different conformational transitions of **9** during HFIP titration. *I*, β-turn; *II*, β-sheet; *III*, α-helix; *IV*, random coil. *d*, snapshots from molecular dynamics simulation of **9**.

severe loss of vitality of neuronal cultures. Monomeric Aβ(1–40) did not induce toxicity on those cultures under the same conditions. The miniamyloids were not submitted to the oligomerization protocol before the treatment of neurons. This was to evaluate their intrinsic ability to induce possible toxic effects on neuronal cultures. We found pairs of miniamyloids bearing comparable characteristics in toxicity pattern of Aβ(1–40), *e.g.* the monomer was non-toxic, whereas the dimer elicited strong toxicity. Some monomeric miniamyloids exhibited toxicity on neurons and were excluded from the study. Because we used the same protocol for preparation of monomers and dimers, we excluded a toxicity induced by buffers or charge pattern of the peptides and hypothesize the induced toxicity to be specific for the peptides.

DISCUSSION

The transient nature of the oligomers of fibril-forming peptides alleviates a structural characterization of low oligomeri-

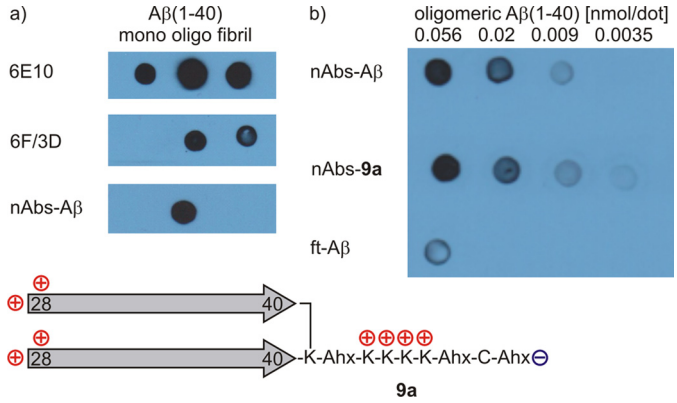

FIGURE 6. *a*, dot blots corresponding to the antibody affinity of different preparations of Aβ(1–40). The antibody 6E10 recognizes Aβ regardless of its aggregation state. The antibody 6F/3D binds oligomeric or fibrillar Aβ but not monomeric Aβ. nAbs-Aβ specifically bind oligomeric Aβ. *b*, affinity chromatography with **9a** yields antibodies (nAbs-**9a**) that bind preparations of oligomeric Aβ with affinities similar to nAbs-Aβ. The flow-through (*ft*-Aβ(1–40)), which are the remaining human antibodies following isolation of nAbs-Aβ from intravenous immunoglobulins (*IVIg*), served as a negative control.

zation degrees (34), thus allowing for speculation about the structure-activity relationships in the case of Aβ oligomers. To devise experiments that differentiate the smallest possible oligomer, a dimeric Aβ peptide from the monomeric single-stranded Aβ peptide was synthesized; we linked two solubilized C-terminal Aβ peptides and investigated the monomers and dimers separately. A fundamental question is the amount of toxicity associated with the degree of oligomerization. From our library of peptides that was investigated, we identified one class of C-terminally linked Aβ dimers that differed considerably from their monomeric counterparts. It is possible to devise a pair of peptides that are non-toxic, not cooperatively folded, and not recognized by nAbs-Aβ in their monomeric form (**5**) but that are toxic, cooperatively folded, and bound by nAbs-Aβ as a dimer (**6**). The pair **8** and **9** is only a minor variation containing additional charged groups. Several other peptides fulfill one or two of the three parameters investigated, but **9** is a candidate for further structural optimization. Current synthetic approaches are aimed to increase the conformational restriction of the epitope. The peptides are promising candidates for the development of sensitive assays for the identification of human nAbs-Aβ in clinical samples. Miniamyloids could be used for active and passive immunization strategies by producing monoclonal antibodies in mice and subsequently humanizing these antibodies for administration in patients.

Solution NMR data indicated that transient soluble forms of Aβ have a mixed parallel and antiparallel β-sheet structure that is different from fibrils (35). Bowers (36) identified the simultaneous occurrence of two different assembly pathways of amyloid-forming peptides, whereas other peptides only form globular aggregates. From the present study, we can expand this view and state that the conformational transition between β-sheet and globular/α-helical structure is a highly cooperative process in the case of Aβ amyloid-type peptides. This finding strengthens the assumed importance of α-helical intermediates during amyloid formation (37, 38). In conclusion, synthetic miniamyloids encompassing the epitope region of Aβ(28–40) and solubilized by the addition of cationic groups to prevent progressive aggregation can mimic the conformational epitope of nAbs-Aβ. They mimic essential features of toxic Aβ while behaving in a manner similar to traditional organic molecules, which are amenable for spectroscopic studies. Therefore, they have possible applications as synthetic epitopes for the isolation of new subgroups of naturally occurring human autoantibodies and are proposed as therapeutic tools, which could provide new vaccination strategies against Alzheimer disease.

Acknowledgments—We thank the Deutsche Forschungsgemeinschaft for financial support and Dr. L. C. Andrei-Selmer and Dr. M. Burg-Roderfeld for technical support.

REFERENCES

1. Jakob-Roetne, R., and Jacobsen, H. (2009) Alzheimer's Disease: From Pathology to Therapeutic Approaches. *Angew. Chem. Int. Ed.* **48,** 3030–3059
2. Selkoe, D. J. (2011) Alzheimer's Disease. *Cold Spring Harb. Perspect. Biol.* **3,** a004457
3. Du, Y., Dodel, R., Hampel, H., Buerger, K., Lin, S., Eastwood, B., Bales, K., Gao, F., Moeller, H. J., Oertel, W., Farlow, M., and Paul, S. (2001) Reduced levels of amyloid b-peptide antibody in Alzheimer disease. *Neurology* **57,** 801–805
4. Du, Y., Wei, X., Dodel, R., Sommer, N., Hampel, H., Gao, F., Ma, Z., Zhao, L., Oertel, W. H., and Farlow, M. (2003) Human anti-β-amyloid antibodies block β-amyloid fibril formation and prevent β-amyloid-induced neurotoxicity. *Brain* **126,** 1935–1939
5. Dodel, R. C., Du, Y., Depboylu, C., Hampel, H., Frölich, L., Haag, A., Hemmeter, U., Paulsen, S., Teipel, S. J., Brettschneider, S., Spottke, A., Nölker, C., Möller, H. J., Wei, X., Farlow, M., Sommer, N., and Oertel, W. H. (2004) Intravenous immunoglobulins containing antibodies against β-amyloid for the treatment of Alzheimer's disease. *J. Neurol. Neurosurg. Psychiatry* **75,** 1472–1474
6. Dodel, R., Balakrishnan, K., Keyvani, K., Deuster, O., Neff, F., Andrei-Selmer, L. C., Röskam, S., Stüer, C., Al-Abed, Y., Noelker, C., Balzer-Geldsetzer, M., Oertel, W., Du, Y., and Bacher, M. (2011) Naturally occurring autoantibodies against β-amyloid: investigating their role in transgenic animal and *in vitro* models of Alzheimer's disease. *J. Neurosci.* **31,** 5847–5854
7. Kayed, R., Head, E., Sarsoza, F., Saing, T., Cotman, C. W., Necula, M., Margol, L., Wu, J., Breydo, L., Thompson, J. L., Rasool, S., Gurlo, T., Butler, P., and Glabe, C. G. (2007) Fibril specific, conformation dependent antibodies recognize a generic epitope common to amyloid fibrils and fibrillar oligomers that is absent in prefibrillar oligomers. *Mol. Neurodegener.* **2,** 18
8. Morgan, C., Colombres, M., Nuñez, M. T., and Inestrosa, N. C. (2004) Structure and function of amyloid in Alzheimer's disease. *Prog. Neurobiol.* **74,** 323–349
9. Takano, K. (2008) Amyloid conformation in aqueous environment. *Curr. Alzheimer Res.* **5,** 540–547
10. Vivekanandan, S., Brender, J. R., Lee, S. Y., and Ramamoorthy, A. (2011) A partially folded structure of amyloid-β(1–40) in an aqueous environment. *Biochem. Biophys. Res. Commun.* **411,** 312–316
11. Takano, K., Endo, S., Mukaiyama, A., Chon, H., Matsumura, H., Koga, Y., and Kanaya, S. (2006) Structure of amyloid b fragments in aqueous environments. *FEBS J.* **273,** 150–158
12. Hoyer, W., Grönwall, C., Jonsson, A., Ståhl, S., and Härd, T. (2008) Stabilization of a β-hairpin in monomeric Alzheimer's amyloid-β peptide inhibits amyloid formation. *Proc. Natl. Acad. Sci. U.S.A.* **105,** 5099–5104
13. Jin, M., Shepardson, N., Yang, T., Chen, G., Walsh, D., and Selkoe, D. J. (2011) Soluble amyloid b-protein dimers isolated from Alzheimer cortex directly induce Tau hyperphosphorylation and neuritic degeneration. *Proc. Natl. Acad. Sci. U.S.A.* **108,** 5819–5824
14. Roychaudhuri, R., Yang, M., Hoshi, M. M., and Teplow, D. B. (2009) Amyloid b-protein assembly and Alzheimer disease. *J. Biol. Chem.* **284,** 4749–4753
15. Schmechel, A., Zentgraf, H., Scheuermann, S., Fritz, G., Pipkorn, R., Reed,

J., Beyreuther, K., Bayer, T. A., and Multhaup, G. (2003) Alzheimer b-Amyloid homodimers facilitate Ab fibrillization and the generation of conformational antibodies. *J. Biol. Chem.* **278,** 35317–35324
16. Yamaguchi, T., Yagi, H., Goto, Y., Matsuzaki, K., and Hoshino, M. (2010) A disulfide-linked amyloid-b peptide dimer forms a protofibril-like oligomer through a distinct pathway from amyloid fibril formation. *Biochemistry* **49,** 7100–7107
17. Müller-Schiffmann, A., Andreyeva, A., Horn, A. H., Gottmann, K., Korth, C., and Sticht, H. (2011) Molecular engineering of a secreted, highly homogeneous, and neurotoxic Ab dimer. *ACS Chem. Neurosci.* **2,** 242–248
18. Kok, W. M., Scanlon, D. B., Karas, J. A., Miles, L. A., Tew, D. J., Parker, M. W., Barnham, K. J., and Hutton, C. A. (2009) Solid-phase synthesis of homodimeric peptides: preparation of covalently-linked dimers of amyloid b peptide. *Chem. Commun. (Camb.)* **12,** 6228–6230
19. Lührs, T., Ritter, C., Adrian, M., Riek-Loher, D., Bohrmann, B., Döbeli, H., Schubert, D., and Riek, R. (2005) 3D structure of Alzheimer's amyloid-b-(1–42) fibrils. *Proc. Natl. Acad. Sci. U.S.A.* **102,** 17342–17347
20. Petkova, A. T., Ishii, Y., Balbach, J. J., Antzutkin, O. N., Leapman, R. D., Delaglio, F., and Tycko, R. (2002) A structural model for Alzheimer's b-amyloid fibrils based on experimental constraints from solid state NMR. *Proc. Natl. Acad. Sci. U.S.A.* **99,** 16742–16747
21. Petkova, A. T., Yau, W. M., and Tycko, R. (2006) Experimental constraints on quaternary structure in Alzheimer's b-amyloid fibrils. *Biochemistry* **45,** 498–512
22. Sato, T., Kienlen-Campard, P., Ahmed, M., Liu, W., Li, H., Elliott, J. I., Aimoto, S., Constantinescu, S. N., Octave, J. N., and Smith, S. O. (2006) Inhibitors of Amyloid Toxicity Based on b-sheet Packing of Ab40 and Ab42. *Biochemistry* **45,** 5503–5516
23. Ahmed, M., Davis, J., Aucoin, D., Sato, T., Ahuja, S., Aimoto, S., Elliott, J. I., Van Nostrand, W. E., and Smith, S. O. (2010) Structural conversion of neurotoxic amyloid-b1–42 oligomers to fibrils. *Nat. Struct. Mol. Biol.* **17,** 561–567
24. Scheidt, H. A., Morgado, I., Rothemund, S., Huster, D., and Fändrich, M. (2011) Solid-state NMR spectroscopic investigation of Ab protofibrils: implication of a b-sheet remodeling upon maturation into terminal amyloid fibrils. *Angew. Chem. Int. Ed.* **50,** 2837–2840
25. Dodel R, Bacher M, Balakrishnan K, Geyer A, and Roeder, A. M. (November 29, 2011) PCT/EP2011/071239
26. Fradinger, E. A., Monien, B. H., Urbanc, B., Lomakin, A., Tan, M., Li, H., Spring, S. M., Condron, M. M., Cruz, L., Xie, C. W., Benedek, G. B., and Bitan, G. (2008) C-terminal peptides coassemble into Ab42 oligomers and protect neurons against Ab42-induced neurotoxicity. *Proc. Natl. Acad. Sci. U.S.A.* **105,** 14175–14180
27. Deleted in proof
28. Walsh, D. M., Hartley, D. M., Kusumoto, Y., Fezoui, Y., Condron, M. M., Lomakin, A., Benedek, G. B., Selkoe, D. J., and Teplow, D. B. (1999) Amyloid b-Protein Fibrillogenesis. *J. Biol. Chem.* **274,** 25945–25952
29. Barrow, C. J., Yasuda, A., Kenny, P. T., and Zagorski, M. G. (1992) Solution conformations and aggregational properties of synthetic amyloid b-peptides of Alzheimer's disease: Analysis of circular dichroism spectra. *J. Mol. Biol.* **225,** 1075–1093
30. Fezoui, Y., and Teplow, D. B. (2002) Kinetic studies of amyloid b-protein fibril assembly. *J. Biol. Chem.* **277,** 36948–36954
31. Tomaselli, S., Esposito, V., Vangone, P., van Nuland, N. A., Bonvin, A. M., Guerrini, R., Tancredi, T., Temussi, P. A., and Picone, D. (2006) The a-to-b conformational transition of Alzheimer's Ab-(1–42) peptide in aqueous media is reversible: a step by step conformational analysis suggests the location of b conformation seeding. *ChemBioChem* **7,** 257–267
32. Greenfield, N. J. (2006) Using circular dichroism collected as a function of temperature to determine the thermodynamics of protein unfolding and binding interactions. *Nat. Protoc.* **1,** 2527–2535
33. Kayed, R., Head, E., Thompson, J. L., McIntire, T. M., Milton, S. C., Cotman, C. W., and Glabe, C. G. (2003) Common Structure of Soluble Amyloid Oligomers Implies Common Mechanism of Pathogenesis. *Science* **300,** 486–489
34. Laganowsky, A., Liu, C., Sawaya, M. R., Whitelegge, J. P., Park, J., Zhao, M., Pensalfini, A., Soriaga, A. B., Landau, M., Teng, P. K., Cascio, D., Glabe, C., and Eisenberg, D. (2012) Atomic view of a toxic amyloid small oligomer. *Science* **335,** 1228–1231
35. Yu, L., Edalji, R., Harlan, J. E., Holzman, T. F., Lopez, A. P., Labkovsky, B., Hillen, H., Barghorn, S., Ebert, U., Richardson, P. L., Miesbauer, L., Solomon, L., Bartley, D., Walter, K., Johnson, R. W., Hajduk, P. J., and Olejniczak, E. T. (2009) Structural characterization of a soluble amyloid β-peptide oligomer. *Biochemistry* **48,** 1870–1877
36. Bleiholder, C., Dupuis, N. F., Wyttenbach, T., and Bowers, M. T. (2011) Ion mobility-mass spectrometry reveals a conformational conversion from random assembly to β-sheet in amyloid fibril formation. *Nat. Chem.* **3,** 172–177
37. Fezoui, Y., Hartley, D. M., Walsh, D. M., Selkoe, D. J., Osterhout, J. J., and Teplow, D. B. (2000) A *de novo* designed helix-turn-helix peptide forms nontoxic amyloid fibrils. *Nat. Struct. Biol.* 7, 1095–1099
38. Hauser, C. A., Deng, R., Mishra, A., Loo, Y., Khoe, U., Zhuang, F., Cheong, D. W., Accardo, A., Sullivan, M. B., Riekel, C., Ying, J. Y., and Hauser, U. A. (2011) Natural tri- to hexapeptides self-assemble in water to amyloid β-type fiber aggregates by unexpected α-helical intermediate structures. *Proc. Natl. Acad. Sci. USA* **108,** 1361–1366